JOURNAL OF THERMOPHYSICS AND HEAT TRANSFER
Vol. 25, No. 1, January–March 2011

Thermal Resistance Analysis of Pin-Fin Heat Sinks Under Nonuniform Impingement Heating

S. S. Feng*
Xi'an Jiaotong University, 710049 Xi'an, People's Republic of China
T. Kim†
University of Witwatersrand, Johannesburg 2050, South Africa
and
T. J. Lu‡
Xi'an Jiaotong University, 710049 Xi'an, People's Republic of China

DOI: 10.2514/1.51520

A thermal resistance analysis for pin-fin heat sinks subjected to nonuniform flame impinging-jet heating is presented. Explicit analytical expression of the overall total resistance is obtained by evaluating each of the individual thermal resistances in the circuit, including the spreading resistance, the material resistance, the convective resistance, and the resistance due to fluid temperature rise. Upon modeling the nonuniform heat flux distribution over the entire upper surface of the substrate due to flame impinging-jet heating with an exponential function, the spreading resistance within a circular plate is obtained analytically. To verify the assumptions/approximations made in the analogy model, the results predicted by the thermal resistance analogy model are compared with those obtained from a three-dimensional numerical model, with overall good agreement achieved. The interaction of heat conduction in the substrate and heat convection in the fluid flow is then investigated using the analogy model. Obtained results demonstrate that increasing the rate of convection heat transfer decreases the spreading resistance in the substrate. Furthermore, an optimal substrate thickness is found to exist when the lateral spreading of heat in the substrate is balanced by that conducted through the thickness direction of the substrate.

Nomenclature

A	=	cross-sectional area of pin fin, m^2
A_b	=	cross-sectional area of substrate, LW, m^2
B, C	=	constants in Eq. (10)
Bi	=	Biot number, $h_e r_0/k_s$
c_p	=	specific heat, J/kg K
D_h	=	hydraulic diameter of pin-fin channel, $2WH/(W+H)$, m
h_b, h_{fin}	=	heat transfer coefficients on substrate and pin fin, W/m^2 K
h_e	=	equivalent endwall heat transfer coefficient, W/m^2 K
$J_0(\cdot)$, $J_1(\cdot)$	=	Bessel functions of order 0 and 1
k	=	thermal conductivity, W/m K
$\dot{m}$	=	mass flow rate of convective flow, kg/s
N	=	number of pin fins
P	=	perimeter of pin fin's cross section, m
Q	=	rate of heat entering into substrate, Eq. (19), W
q_0	=	heat flux level at impinging center, W/m^2 K
R_{conv}	=	equivalent convection resistance, K/W
R_{film}	=	film resistance at unfinned substrate surface, K/W
R_{fin}	=	fin resistance, K/W
R_{heat}	=	resistance caused by fluid temperature rise, K/W
R_m	=	material resistance, K/W
R_s	=	spreading resistance, K/W
R_{sub}	=	substrate resistance, $R_s + R_m$, K/W
R_{tot}	=	total thermal resistance, K/W
Re_{Dh}	=	convection Reynolds number based on hydraulic diameter, $\rho_{\text{in}} u_0 D_h/\mu_{f,\text{in}}$
r_0	=	equivalent radius of rectangular substrate, Eq. (7), m
$T_{f,\text{ave}}$	=	average fluid temperature, K
T_{in}	=	inlet temperature of convective flow, K
$\bar{T}_{\text{up}}$, $\bar{T}_{\text{low}}$	=	average temperature over upper surface and lower surface, K
T_0	=	centroid temperature at impinging center, K
t	=	thickness of substrate, m
u_0	=	approach velocity of convective flow, m/s
μ	=	viscosity, kg/ms
θ	=	temperature rise of substrate, $T_b(r,z) - T_{f,\text{ave}}$, K
λ_n	=	dimensionless eigenvalues
Ψ_s	=	dimensionless spreading resistance, $k_s r_0 R_s$, Eq. (20)
Ψ_{sub}	=	dimensionless substrate resistance, $k_s r_0 R_{\text{sub}}$, Eq. (47)
ρ	=	density, kg/m^3
τ	=	dimensionless substrate thickness, t/r_0

Subscripts

b	=	substrate
f	=	fluid
fin	=	pin fin
s	=	solid

Received 8 July 2010; revision received 30 September 2010; accepted for publication 2 October 2010.

*Ph.D. Student, School of Energy and Power Engineering; shangshengf@gmail.com.
†Associate Professor, School of Mechanical, Industrial and Aeronautical Engineering; tong.kim@wits.ac.za.
‡Professor, Ministry of Education Key Laboratory for Strength and Vibration, School of Aerospace; tjlu@mail.xjtu.edu.cn (Corresponding Author).

I. Introduction

PIN fins have been extensively used in a wide range of industrial applications, such as internal cooling of turbine blades, thermal management of power electronics, and compact heat exchangers. Correspondingly, numerous studies have been carried out to explore the thermal and fluidic mechanisms associated with pin-fin arrays in

forced convection. The majority of these studies focus on pin-fin heat sinks with *uniform thermal boundary* (either temperature or heat flux) conditions imposed through the substrate to which the pin fins are attached [1–5].

In certain engineering applications, e.g., jet blast deflector (JBD), in which a flat panel accommodating a specially designed heat exchanger deflects exhaust gas from a jet engine, the thermal boundary conditions imposed on the JBD cannot be described as uniform. Motivated by this engineering application, this work deals with single-phase forced convection in pin-fin heat sinks subjected to nonuniform heating that mimics a flame jet impinging normally on a simplified JBD setup, as shown schematically in Fig. 1.

To assess the performance of a heat exchanger for practical applications, theoretical modeling plays an important role. With the rapid progress of high-speed computers, numerical simulations such as computational fluid dynamics (CFD) have been successfully implemented for many applications. However, for the present problem shown in Fig. 1, the CFD simulations can be computationally intensive, since several millions of elements are needed to fully realize the flow characteristics around pin-fin geometries and are hence time-consuming; furthermore, the prediction accuracy is often challenging when turbulence in pin-fin geometries needs to be modeled. To avoid modeling the time-consuming and challenging turbulent flow in the pin fins, the present authors have analytically developed and experimentally validated a numerical model for pin-fin heat sinks under nonuniform hot-gas impinging-jet heating [6]. The fluid flow was assumed to have a uniform temperature within each pin-fin unit cell so that the in-plane distribution of fluid temperature can be predicted without knowing the local flow distribution in each unit. The equations governing fluid flow temperature, substrate temperature, pin-fin temperature were coupled to solve. Nonuniform convective heating boundary condition was applied at the top surface of the substrate to model the heating of hot-gas impinging jet. Empirical heat transfer coefficients were applied over pin-fin surfaces and unfinned substrate surface in the channel. However, to solve the numerical model in [6], a complicated computer program is still required. It is therefore valuable to develop a simplified yet accurate analytical model for engineering-level modeling of the problem shown in Fig. 1.

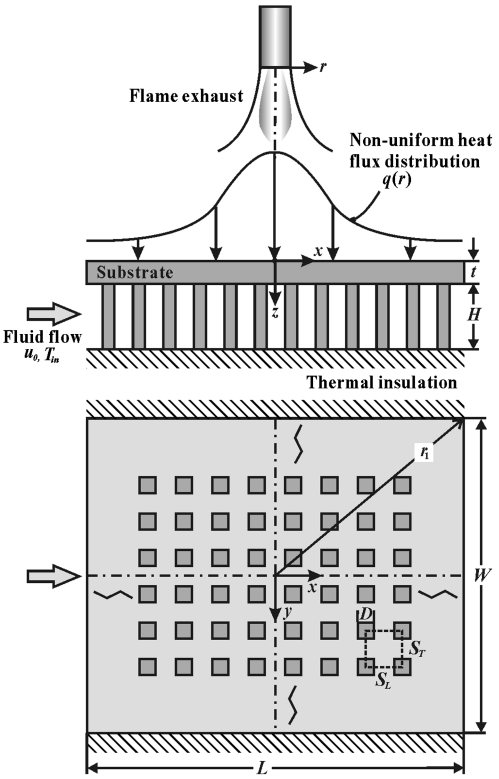

Fig. 1 Pin-fin heat sink subjected to nonuniform flame impinging-jet heating.

The thermal resistance analogy has been employed in lieu of numerical simulation to predict the overall thermal performance of a pin-fin heat sink under uniform and nonuniform heating conditions [7,8]. Under a uniform heat flux boundary condition, Peles et al. [7] performed thermal resistance analysis for a micro pin-fin heat sink, and only the convective resistance and the resistance caused by fluid temperature rise were included in the circuit. They found that the thermal resistance caused by fluid temperature rise plays an important role in the total thermal resistance for a micro pin-fin heat sink, whereas the material resistance in the substrate is negligible. For electronics cooling with localized (or discrete) nonuniform heating, Khan et al. [8] developed a thermal resistance model to calculate the heat source temperature. The source-to-baseplate joint resistance, spreading resistance, material resistance, baseplate-to-pin contact resistance, and convective resistance were included in the circuit. The spreading resistance was determined from previous studies (Yovanovich et al. [9] and Song et al. [10]).

Unlike numerical simulation such as CFD predicting the local thermal field at every point in the heat sink, the thermal resistance analogy only focus on some special temperatures at selected locations (or joints) in the heat sink, these temperatures are connected by thermal resistance network. By determining the expressions of each individual thermal resistances, the concerning temperatures at selected locations can then be determined. This simplification offers the merits for the thermal resistance analogy: simply, explicit analytical expressions for complex engineering problem can be obtained without tedious numerical simulation.

One objective of this paper is to develop a simple yet accurate model for engineering-level modeling of pin-fin heat sinks subjected to nonuniform flame impinging-jet heating from the spreading resistance perspective. Heating by the flame impinging jet is modeled by prescribing a nonuniform heat flux distribution expressed by an exponential function on the substrate. To determine the overall system resistance of heat sink, the spreading resistance of continuous nonuniform exponential heat flux distribution on finite circular plate is presented. The assumptions/approximations made in the thermal resistance analogy are verified by comparing the results with those obtained from a previously developed numerical model in [6]. Based on the verified model, the second objective is to analyze the effects of convective flow rate and thermal conductivity of material on variation of each individual thermal resistance. Particular analysis is made on the interaction of spreading resistance in the substrate and convection resistance in fluid flow. The optimal substrate thickness that minimizes temperature at the impinging center at given flow condition is also revealed and analyzed in detail.

II. Review of Spreading Resistance for Electronics Cooling

Constriction and spreading resistances exist whenever heat is transferred from one region to another with a cross-sectional area change. When heat flows from a small source area to a large space, the thermal resistance is called spreading resistance, inversely when heat enters a small cross-sectional area from a large space, the thermal resistance is called constriction resistance [11]. Constriction/spreading resistances are often involved in electronic packaging design, and hence extensive studies have been devoted to this field for many different geometries (e.g., circular plate, rectangular plate, half-space, etc.) and different boundary conditions.

Lee et al. [12] investigated heat spreading in finite isotropic circular plate of radius b and thickness t with a circular isoflux heat source of radius a over a portion of the upper surface ($z = 0$). The remainder upper surface outside the source and the side surface were adiabatic. Uniform heat transfer coefficient (or contact conductance) h_e and fixed reference temperature T_f were specified at the lower surface of the plate, as schematically shown in Fig. 2a. They presented analytical solutions for dimensionless spreading resistances based on both centroid temperature and source average temperature in the form of infinite series.

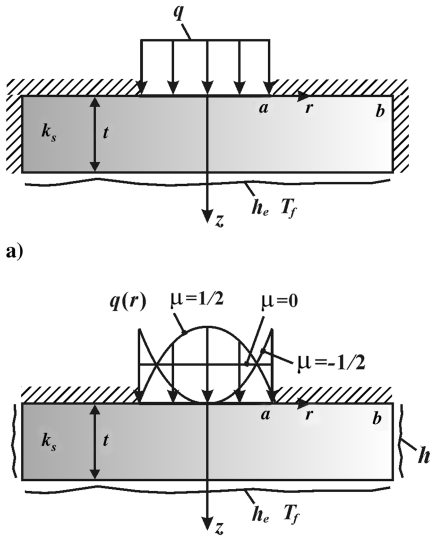

Fig. 2 Spreading resistance of circular heat source on finite circular plate: a) isoflux over source area and b) axisymmetric heat flux over source area.

Song et al. [10] provided simple closed form correlation equations for the exact solution developed in [12]. The correlation equations were within 10% of the exact solution. An example analysis was performed to demonstrate the usefulness of the equations. In their case study, a fin heat sink was tested under two boundary conditions separately: isoflux over the entire substrate surface and isoflux over partial central area of the substrate surface (i.e., uniform heating vs discrete nonuniform heating). The equivalent heat transfer coefficient h_e was measured from the uniform heating measurement. Then it was used in the spreading resistance model to predict the temperature of heat sink with discrete heating condition. The predicted results agreed well with those from the discrete heating measurements.

Kennedy [13] solved temperature distributions in finite circular plate with circular isoflux heat source over portion of the upper surface. Three boundary condition combinations were investigated by considering whether it was adiabatic or at a constant temperature for the side surface and the lower surface of the plate. The spreading resistance was not presented explicitly, and the nondimensional temperature within the circular plate nondimensionalized by the centroid temperature was plotted in the paper: i.e., $T_b(r,z)/T_b(0,0)$.

Lu et al. [14] developed analytical models for temperature distributions in single layer circular plate and two-layer circular plate with isothermal circular heat source that is positioned over the central portion of the upper surface of the plate. The shear-lag type method was used to solve the governing equations, which led to simple solutions without any infinite series. Through analyzing the obtained results, the authors were able to demonstrate both the spreading effects and the insulation effects of the substrate, depending on the chip-level power density, chip density (spacing), material of the substrate, etc.

In addition to isoflux and isothermal boundary conditions considered, the spreading resistances for general, axisymmetric heat flux distribution $q(r)$ over the circular source have been also investigated by numerous researchers. Yovanovich [15] presented general solution for thermal spreading and system resistances of a circular source of radius a on a finite circular plate of radius b and thickness t. The side surface and the lower end surface were cooled by fluid flow with individual heat transfer coefficients along each surface, while at a fixed reference temperature, as schematically shown in Fig. 2b. The axisymmetric heat flux distribution has the form as

$$q(r) = \frac{Q(1+\mu)}{\pi a^2}\left[1 - \left(\frac{r}{a}\right)^2\right]^{\mu} \quad \text{for } 0 < \frac{r}{a} < 1 \tag{1}$$

where μ is the heat flux distribution parameter. Three particular solutions were considered by setting: $\mu = -1/2$, the equivalent isothermal source (as this distribution produces nearly isothermal condition on surface area); $\mu = 0$, isoflux source; and $\mu = 1/2$, parabolic flux distribution (see Fig. 2b).

Yovanovich et al. [16] obtained spreading resistance within a two-layer circular plate of radius b. A general heat flux distribution was applied over a circular source of radius a situated centrally on the upper surface of the compound plate, with the form of $q(r) = q_0[1-(r/a)^2]^{\mu}$, where q_0 is the heat flux level at the centroid of the source. The remainder of the upper surface outside the source was adiabatic, the lower end surface was subjected to convective cooling (h_e, T_f), and two boundary conditions were considered along the side surface: constant temperature and adiabatic.

Mikic and Rohsenow [17] also reported spreading resistances for general heat flux distribution over a circular heat source on one end of a semi-infinite circular plate and a finite circular plate with the adiabatic side surface. Through analysis they found that the spreading resistance can be obtained by means of the alternative definition (based on source average temperature):

$$QR_s = \frac{2}{a^2}\int_0^a T_b(r,0)\,r\,\mathrm{d}r - \frac{2}{b^2}\int_0^b T_b(r,0)\,r\,\mathrm{d}r \tag{2}$$

where $T_b(r,0)$ is axisymmetric temperature on the source plane $z = 0$.

Yovanovich et al. [9] presented analytical models for spreading resistance of an isoflux, rectangular heat source on a two-layer rectangular plate with convective cooling boundary at the lower end surface. The spreading resistance within rectangular plate is substantially three-dimensional, while several investigators have argued that the 3-D spreading models can be simplified by using the 2-D axisymmetric model in circular plate if appropriate length scale is used in the nondimensional spreading resistance (Negus et al. [18], Nelson and Sayers [19], and Naraghi and Antonetti [20]).

Negus et al. [18] showed that when the square root of the source area is selected as length scale to nondimensionalize the spreading resistance and the ratio of source area to cross-sectional area of the conducting plate are the same, then such defined nondimensional spreading resistances have very close values for circle/circle, circle/square and square/square source-to-plate combinations.

Nelson and Sayers [19] numerically compared the spreading resistances within 2-D planar, axisymmetric plate, and rectangular plate. The influence of the aspect ratio of the rectangular plate was examined. They concluded that the axisymmetric model is always accurate to replace 3-D model with aspect ratios near one.

As reviewed above, numerous studies have been devoted to the spreading resistances extensively for electronic cooling application, where *discrete nonuniform heating* at a boundary surface is involved (i.e., the heat source area is smaller than the cross-sectional area of the substrate). In comparison, for present problem, as shown in Fig. 1, the substrate of heat sink is subjected to a *continuous nonuniform heat flux* expressed by exponential function due to the flame impinging-jet heating (i.e., the heat source over the entire substrate surface but being nonuniform). To the best of our knowledge, there is no readily available spreading resistance model for the present problem, although it may be obtained by considering the limiting case of the existing solutions for axisymmetric heat flux distribution over circular source area on finite circular plate. The spreading resistance of continuous nonuniform exponential heat flux distribution on finite circular plate is therefore reported in the study to determine the overall system resistance of a heat sink subjected to flame impinging-jet heating.

III. Thermal Resistance Model

Consider pin-fin heat sink subjected to nonuniform exponential heat flux distribution $q(r)$ due to flame impinging jet, as shown schematically in Fig. 1. The dimensions of the heat-sink substrate are length L by width W by thickness t. The pin fins are monolithically rooted from the substrate and there is no contact resistance between

them assumed. The pin-fin array is inline arranged, and each pin-fin element is square-shaped, with cross-sectional area of $A = D^2$ and height H, whereas the thermal analogy model developed below is not limited to square pin fins and inline arrangement. The transverse and longitudinal center-to-center pin pitches are S_T and S_L, respectively. Uniform and steady flow of air coolant is forced passing through the channel to remove the heat from jet. The approach velocity of the fluid is u_0 with a temperature T_{in}. Assume that the side surfaces of the substrate and that of the flow channel and the bottom substrate of the flow channel are all adiabatic.

A. Overall Total Thermal Resistance

An analogy between the present pin-fin heat sink under flame impinging jet and that with discrete heat source for electronics cooling can be made, as illustrated in Fig. 3. For the present problem of Fig. 3a, the flame impinging jet produces a *continuous nonuniform exponential heat flux* over the entire upper surface $z = 0$; for the problem of Fig. 3b, *discrete nonuniform heat flux* is applied over the central area of the upper surface, the rest of the upper surface area being adiabatic. Common for both cases, the nonuniform heat flux distribution causes lateral heat spreading in the substrate and, after spreading, all the heat sources leave the substrate at $z = t$ and finally end up in the fluid. Because of the similarity of the two problems, the thermal analogy model of the present problem can be developed based on the model established by Khan et al. [8] and Culham et al. [21] for electronics cooling, as detailed below.

The overall total thermal resistance in the study is defined based on the centroid temperature rise, as

$$R_{\text{tot}} = \frac{T_0 - T_{\text{in}}}{Q} \tag{3}$$

where T_0 is the substrate temperature at the impinging center, Q is the rate of heat transfer from the jet. The total thermal resistance is composed of several individual thermal resistances, i.e., spreading resistance R_s, material resistance R_m, equivalent convective resistance R_{conv}, and thermal resistance caused by fluid temperature rise R_{heat} (see Fig. 4), as,

$$R_{\text{tot}} = R_s + R_m + R_{\text{conv}} + R_{\text{heat}} \tag{4}$$

and

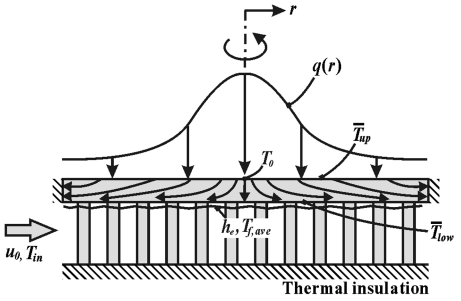

a)

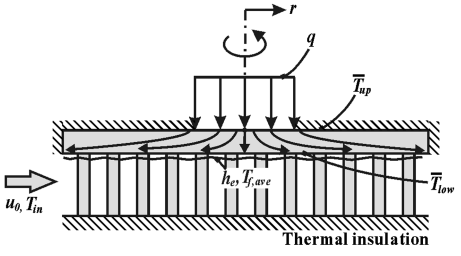

b)

Fig. 3 Analogy between a) heat sink under flame impinging jet and b) heat sink with discrete heat source in electronics cooling.

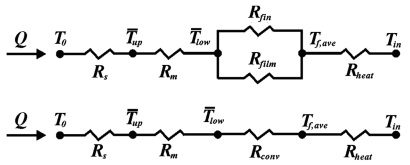

Fig. 4 Thermal resistance circuit for heat sink subjected to nonuniform flame impinging jet.

$$R_{\text{conv}} = 1/[N/R_{\text{fin}} + 1/R_{\text{film}}] \tag{5}$$

The definitions of the each individual thermal resistance are

$$R_s = \frac{T_0 - \bar{T}_{\text{up}}}{Q} \tag{6a}$$

$$R_m = \frac{\bar{T}_{\text{up}} - \bar{T}_{\text{low}}}{Q} \tag{6b}$$

$$R_{\text{conv}} = \frac{\bar{T}_{\text{low}} - T_{f,\text{ave}}}{Q} \tag{6c}$$

$$R_{\text{heat}} = \frac{T_{f,\text{avg}} - T_{\text{in}}}{Q} \tag{6d}$$

where $\bar{T}_{\text{up}}$ and $\bar{T}_{\text{low}}$ are the substrate temperature averaged over the surface at $z = 0$ and $z = t$, respectively, and $T_{f,\text{ave}}$ is the average temperature of fluid over the entire pin-fin channel. Substitution of Eqs. (6a–6d) into Eq. (4) reduces to the definition of the total thermal resistance: i.e., Eq. (3).

Note that in present thermal resistance circuit shown in Fig. 4, only the macro-spreading resistance in the substrate due to the applied nonuniform heat flux on the upper surface $z = 0$ is included; in fact, there is also additional constriction resistance existing in each pin-fin unit cell as heat entering pin fins from the substrate. Compared with the macro-spreading resistance, the constriction resistance is a local thermal behavior and expected to be minor especially when the pin network is dense and the conductivity of material is high. The error caused by ignoring the local constriction resistance can be estimated using the numerical model described in Sec. IV.

B. Spreading Resistance

To obtain the spreading resistance, heat conduction in the substrate of heat sink is separately considered. The cross-sectional area of the substrate is actually rectangular (see Fig. 1). To simplify the problem, an axisymmetric model is considered instead of the rectangular substrate, as shown in Fig. 5. The circular plate has a radius r_0, thickness t, thermal conductivity k_s, and is isotropic. An axisymmetric heat flux distribution $q(r)$ expressed by exponential function is applied over the upper surface of the substrate $z = 0$ to simulate the heating of flame impinging jet. At the lower surface ($z = t$) a uniform heat transfer coefficient h_e and a fixed fluid temperature $T_{f,\text{ave}}$ are

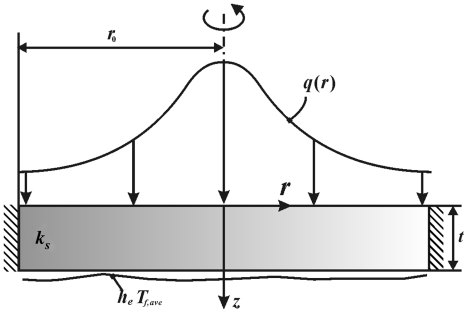

Fig. 5 Spreading resistance of nonuniform exponential heat flux on circular plate with convective cooling.

applied, whereas the side surface $r = r_0$ is adiabatic. Note that the heat transfer coefficient h_e is an equivalent endwall heat transfer coefficient, which considers the elevation of heat transfer by pin fins. The determination of h_e will be addressed later.

According to the findings of Negus et al. [18], Nelson and Sayers [19], and Naraghi and Antonetti [20], the spreading resistance in circular plate can effectively represent that of rectangular plate, given that the equivalent radius of the rectangular plate is the same as the radius of the circular plate. The equivalent radius of the rectangular plate is therefore calculated as (see Figs. 1 and 5):

$$r_0 = \sqrt{\frac{A_b}{\pi}} = \sqrt{\frac{LW}{\pi}} \tag{7}$$

The governing differential equation for the temperature distribution in the circular plate is

$$\frac{1}{r}\frac{\partial}{\partial r}\left(r\frac{\partial\theta}{\partial r}\right) + \frac{\partial^2\theta}{\partial z^2} = 0 \qquad 0 < r < r_0, \qquad 0 < z < t \tag{8}$$

The boundary conditions are

$$\frac{\partial\theta}{\partial r} = 0 \quad \text{at } r = 0 \tag{9a}$$

$$\frac{\partial\theta}{\partial r} = 0 \quad \text{at } r = r_0 \tag{9b}$$

$$-k_s\frac{\partial\theta}{\partial z} = q(r) \quad \text{at } z = 0 \tag{9c}$$

$$-k_s\frac{\partial\theta}{\partial z} = h_e\theta \quad \text{at } z = t \tag{9d}$$

where $\theta(r, z) = T_b(r, z) - T_{f,\text{ave}}$ is the temperature rise, $T_b(r, z)$ is the substrate temperature.

In Eq. (9c), the nonuniform heat flux distribution due to flame jet can be expressed by an exponential function as [22,23]:

$$q(r) = q_0 e^{-B(r/r_1)^C} \tag{10}$$

where B and C are the constants adjusting the distribution shape; q_0 is the maximum heat flux at the impinging center, i.e., at $(r, z) = (0, 0)$; and r_1 is the radial distance from corners of the rectangular substrate to the impinging center (see Fig. 1). For a given flame jet configuration, the constants can be determined by a hybrid numerical-experimental analysis. Equation (10) for rectangular substrate is converted to the form for circular substrate, as

$$q(r) = q_0 e^{-B_1(r/r_0)^C} \tag{11}$$

and

$$B_1 = B(r_0/r_1)^C = B\left(\sqrt{\frac{4}{\pi}\cdot\frac{\beta}{\beta^2+1}}\right)^C \tag{12}$$

where $\beta = L/W$ is the aspect ratio of the rectangular substrate.

Upon applying the method of separation of variables, the solution of the temperature distribution in the substrate can be obtained, as

$$\theta(r, z) = 2\frac{q_0 r_0}{k_s}\left[\int_0^1 \gamma e^{-B_1\gamma^C}\,\mathrm{d}\gamma\left(\tau - \zeta + \frac{1}{Bi}\right) + \sum_{n=1}^{\infty}\frac{\int_0^1 \gamma e^{-B_1\gamma^C} J_0(\lambda_n\gamma)\mathrm{d}\gamma J_0(\lambda_n\gamma)\phi_n}{\lambda_n J_0^2(\lambda_n)}\right] \tag{13}$$

where

$$\phi_n = \frac{\lambda_n\cosh(\lambda_n(\tau-\zeta)) + Bi\sinh(\lambda_n(\tau-\zeta))}{\lambda_n\sinh(\lambda_n\tau) + Bi\cosh(\lambda_n\tau)} \tag{14}$$

Here, $\tau = t/r_0$, $\gamma = r/r_0$, $\zeta = z/r_0$; $J_0(\cdot)$ and $J_1(\cdot)$ are the Bessel functions of the first kind of order 0 and 1; and the eigenvalue λ_n are the roots of $J_1(\lambda_n) = 0$ which are computed by means of the following modified Stokes approximation [15]:

$$\lambda_n = \frac{\beta_n}{4}\left[1 - \frac{6}{\beta_n^2} + \frac{6}{\beta_n^4} - \frac{4716}{5\beta_n^6} + \frac{3902918}{70\beta_n^8}\right] \tag{15}$$

with $\beta_n = \pi(4n + 1)$ and $n = 1, 2, 3, \ldots$

The Biot number Bi is defined as

$$Bi = \frac{h_e r_0}{k_s} \tag{16}$$

The substrate temperature at the impinging center and the average temperature over the upper surface $z = 0$ are determined as

$$T_0 = \theta(0, 0) + T_{f,\text{ave}} \tag{17}$$

$$\bar{T}_{\text{up}} = \frac{2\pi}{A_b}\int_0^{r_0} r(\theta(r, 0) + T_{f,\text{ave}})\,\mathrm{d}r \tag{18}$$

The rate of heat entering into the substrate from jet can be obtained by integrating the local heat flux distribution $q(r)$ as

$$Q = 2\pi\int_0^{r_0} rq(r)\,\mathrm{d}r \tag{19}$$

According to Eq. (6a), the spreading resistance can be finally determined with its dimensionless form as

$$\Psi_s = k_s r_0 R_s = \frac{1}{\pi}\sum_{n=1}^{\infty}\frac{\int_0^1 \gamma e^{-B_1\gamma^C} J_0(\lambda_n\gamma)\,\mathrm{d}\gamma\phi_n'}{\lambda_n J_0^2(\lambda_n)\int_0^1 \gamma e^{-B_1\gamma^C}\,\mathrm{d}\gamma} \tag{20}$$

where

$$\phi_n' = \frac{\lambda_n\cosh(\lambda_n\tau) + Bi\sinh(\lambda_n\tau)}{\lambda_n\sinh(\lambda_n\tau) + Bi\cosh(\lambda_n\tau)} \tag{21}$$

C. Material Resistance

The material resistance, along with the spreading resistance, is associated with heat conduction in the substrate. The material resistance exists along the thickness direction of the substrate and can be directly determined using Fourier's law, as

$$R_m = \frac{t}{A_b k_s} \tag{22}$$

D. Equivalent Convective Thermal Resistance

At the lower surface of the substrate ($z = t$), part of the heat is taken away directly by fluid flow from the unfinned surface area, and the associated convective resistance is the film resistance R_{film} [8,21]. The remaining heat is conducted by pin fins and finally convected at the pin-fin surfaces, the thermal resistance is associated with conduction along the pin height, and convection at the pin-fin surface is the fin resistance R_{fin} [8,21]. The equivalent convective thermal resistance assumes that all the heat is dissipated to fluid flow at the bottom surface of the substrate (area $A_b = LW$) by convection with an equivalent endwall heat transfer coefficient h_e and fixed average fluid temperature $T_{f,\text{ave}}$. Therefore, the following expression for R_{conv} is equivalent to that of Eq. (5), as

$$R_{\text{conv}} = \frac{1}{h_e A_b} \tag{23}$$

The equivalent endwall heat transfer coefficient can be obtained by experimental measurements with uniform boundary conditions [10] or determined by empirical correlations. Upon the assumption of uniform equivalent endwall heat transfer coefficient of the pin-fin

channel flow, an arbitrary unit cell of the pin-fin heat sink (see Fig. 6) can be used to determine h_e. Heat balance for the substrate in the unit cell dictates

$$Q^u = Q_b^u + Q_{\text{fin}}^u \tag{24}$$

where

$$Q^u = h_e(S_T S_L)(\bar{T}_b - T_f) \tag{25}$$

$$Q_b^u = h_b(S_T S_L - A)(\bar{T}_b - T_f) \tag{26}$$

$$Q_{\text{fin}}^u = h_{\text{fin}}\eta_{\text{fin}}(PH)(\bar{T}_b - T_f) \tag{27}$$

where Q^u, Q_b^u, and Q_{fin}^u are the total rate of heat dissipation in the unit cell, heat convection from the unfinned surface in the unit cell, and heat dissipation from pin fin in the unit cell, respectively; $\bar{T}_b$ is the average temperature of the substrate at surface $z = t$ in the unit cell; T_f is the average fluid temperature in the unit cell; A and P are the cross-sectional area and perimeter of the pin fin, respectively; h_b is the heat transfer coefficient on the substrate surface (unfinned surface) directly exposed to the convective flow, and h_{fin} is that on the pin-fin surface; and η_{fin} is the fin efficiency given by

$$\eta_{\text{fin}} = \frac{\tanh(mH)}{mH} \tag{28}$$

$$m = \sqrt{\frac{h_{\text{fin}}P}{k_s A}} \tag{29}$$

Substitution of Eqs. (25–27) into Eq. (24), one can obtain the equivalent endwall heat transfer coefficient as

$$h_e = \frac{h_b(S_T S_L - A) + h_{\text{fin}}\eta_{\text{fin}}(PH)}{(S_T S_L)} \tag{30}$$

In Eq. (30), the heat transfer coefficient h_{fin} for square pin fins has been empirically correlated by Kim et al. [4], and the heat transfer coefficient h_b may be taken as $h_b = h_{\text{fin}}$ as suggested by Feng et al. [6].

E. Thermal Resistance Caused by Fluid Temperature Rise

According to the definition in Eq. (6d), the thermal resistance caused by fluid temperature rise can be determined if the average fluid temperature in the channel is known. The average fluid temperature $T_{f,\text{ave}}$ is approximately estimated by considering energy balance of fluid flow across the channel from inlet to outlet, as

$$Q = \dot{m}c_p(T_{\text{out}} - T_{\text{in}}) \tag{31}$$

where $\dot{m}$ is the mass flow rate of the convective flow, and T_{in} and T_{out} are the bulk mean temperature of fluid at the inlet and exit of the pin-fin array, respectively. Assuming that the average fluid temperature in the pin-fin channel takes the arithmetic mean of T_{in} and T_{out}, one has

$$T_{f,\text{ave}} \cong \frac{(T_{\text{out}} + T_{\text{in}})}{2} = \frac{Q}{2\dot{m}c_p} + T_{\text{in}} \tag{32}$$

Substitution of Eq. (32) into Eq. (6d) yields the thermal resistance caused by fluid temperature rise as

$$R_{\text{heat}} \cong \frac{1}{2\dot{m}c_p} \tag{33}$$

Finally, the analytical expression for the total thermal resistance is determined by adding the each resistance serially:

$$R_{\text{tot}} = \frac{\Psi_s}{k_s r_0} + \frac{t}{k_s A_b} + \frac{1}{h_e A_b} + \frac{1}{2\dot{m}c_p} \tag{34}$$

IV. Numerical Model

In the proposed analogy model, a few assumptions/approximations have been made to simplify the problem:

1) The fluid temperature $T_{f,\text{ave}}$ is assumed to be uniform beneath the substrate in the channel, whereas it is spatially distributed in reality.

2) A circular plate is used instead of the rectangular plate.

3) The average fluid temperate over the pin-fin channel is approximated by taking the arithmetic mean of fluid temperatures at the inlet and outlet when determining R_{heat}.

4) The constriction resistance in the substrate near each pin-fin end due to heat entering pin fins from the substrate is not taken into consideration; i.e., local thermal behavior near pin-fin roots in each unit cell is not considered.

As it has been established that the numerical model developed by the present authors in [6] is able to predict the coupled 3-D local temperature fields in the substrate, in the fluid, and in each pin fin, it is therefore free from all the assumptions/approximations made in the analogy model as listed above. Actually, the numerical model was developed analytically; the name semi-empirical model used in [6] is due to the fact that the model needs empirical correlations for heat transfer coefficients on pin surfaces (h_{fin}) and on the unfinned substrate surface (h_b). Therefore, the numerical model can be employed here to check the accuracy of the present analogy model. For completeness, the numerical model is briefly described below; more details can be found in [6].

A. Heat Conduction in Substrate

The temperature field in the substrate $T_b(x, y, z)$ is governed by 3-D heat conduction equation, as

$$(\rho c_p)_s \frac{\partial T_b(x,y,z)}{\partial \tau} = k_s\left(\frac{\partial^2 T_b(x,y,z)}{\partial x^2} + \frac{\partial^2 T_b(x,y,z)}{\partial y^2} + \frac{\partial^2 T_b(x,y,z)}{\partial z^2}\right) \tag{35}$$

For the present pin-fin heat sink (Fig. 1), the boundary conditions for Eq. (35) are specified as follows.

On side edges ($x = \pm L/2$, $y = W/2$) and symmetry surface ($y = 0$),

$$\frac{\partial T_b}{\partial x} = 0 \quad \text{at } x = \pm L/2 \tag{36a}$$

$$\frac{\partial T_b}{\partial y} = 0 \quad \text{at } y = 0, \quad \text{and } y = W/2 \tag{36b}$$

On the substrate surface at $z = 0$,

$$-k_s \frac{\partial T_b}{\partial z} = q(r) \tag{36c}$$

On the substrate surface at $z = t$ directly exposed to fluid flow,

$$-k_s \frac{\partial T_b(x,y,z)}{\partial z} = h_b(T_b(x,y,t) - T_f(x,y)) \tag{36d}$$

On the substrate surface at $z = t$ connected to pin fins,

$$-k_s \frac{\partial T_b(x,y,z)}{\partial z} = q_{\text{fin}} \tag{36e}$$

where $T_f(x, y)$ is the averaged fluid temperature in the pin-fin unit (to be defined later), and q_{fin} is the heat flux conducted by the pin fin from the substrate. A positive q_{fin} indicates that heat transfer occurs from the substrate to the pin fin. Note that the value of q_{fin} for each pin fin differs, depending on its spatial location.

B. Energy Equation for Forced Convective Flow

With the assumption of uniform fluid temperature in each unit cell, the variation of the (average) fluid temperature in the x-y plane can be obtained by heat balance analysis of fluid flow within an arbitrary located unit cell (Fig. 6). It has been established that, with the four heat transfer mechanisms (heat storage, conduction, streamwise convection, and heat source), the differential equation governing the distribution of the unit-cell-averaged fluid temperature in the x-y plane is given by [6]

$$(\rho c_p)_f\left(\frac{\partial T_f(x,y)}{\partial \tau}+u_0\frac{\partial T_f(x,y)}{\partial x}\right) = k_f\left(\frac{\partial^2 T_f(x,y)}{\partial x^2}+\frac{\partial^2 T_f(x,y)}{\partial y^2}\right)+\dot{q} \tag{37}$$

where $\dot{q}$ is the heat source due to heat dissipation from the substrate and the pin fin to the fluid flow:

$$\dot{q}=\frac{Q_b^u+Q_{\text{fin}}^u}{S_T S_L H} \tag{38}$$

and

$$Q_b^u = h_b(S_T S_L - A)(\bar{T}_b(x,y,t)-T_f(x,y)) \tag{39}$$

$$Q_{\text{fin}}^u = h_{\text{fin}} PH(\bar{T}_{\text{fin}}-T_f(x,y)) \tag{40}$$

Here, $\bar{T}_b(x,y,t)$ is the average temperature of the substrate over the unfinned surface in the unit cell, and $\bar{T}_{\text{fin}}$ is the pin-fin temperature averaged over the unit cell (to be determined later).

The boundary conditions for Eq. (37) are

$$T_f = T_{\text{in}} \quad \text{at } x=-L/2 \tag{41a}$$

$$\frac{\partial T_f}{\partial x}=\frac{\partial T_f}{\partial y}=0 \quad \text{at } x=L/2,\ y=0, W/2 \tag{41b}$$

C. Fin Analogy

To determine the heat flux conducted to each pin fin from the substrate, i.e., q_{fin} in Eq. (36e), and its subsequent dissipation to the convective flow, i.e., Q_{fin}^u in Eq. (40), the transfer of heat in each pin fin is considered by adopting the classical fin analogy, as

$$(\rho c_p)_s\frac{\partial T_{\text{fin}}(\zeta)}{\partial \tau}=k_s\frac{\partial^2 T_{\text{fin}}(\zeta)}{\partial \zeta^2}-\frac{h_{\text{fin}}P}{A}(T_{\text{fin}}(\zeta)-T_f(x,y)) \tag{42}$$

where ζ is the local coordinate along the pin-fin height, as illustrated in Fig. 6.

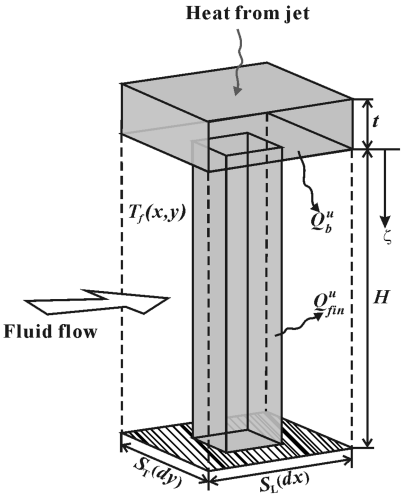

Fig. 6 Heat balance in a representative unit cell of pin-fin heat sink.

Equation (42) can be solved subjected to the following boundary conditions. At the root of each pin fin, its temperature is identical to that of the substrate:

$$T_{\text{fin}}(\zeta)|_{\zeta=0}=T_b(x,y,t) \tag{43a}$$

The tip of the pin fin is thermally insulated:

$$\left.\frac{\partial T_{\text{fin}}(\zeta)}{\partial \zeta}\right|_{\zeta=H}=0 \tag{43b}$$

Once $T_{\text{fin}}(\zeta)$ is determined, heat conducted to the pin fin from the substrate can be calculated as

$$q_{\text{fin}}=-k_s\left.\frac{\partial T_{\text{fin}}(\zeta)}{\partial \zeta}\right|_{\zeta=0} \tag{44}$$

and the average pin-fin temperature appearing in Eq. (40) is

$$\bar{T}_{\text{fin}}=(1/H)\int_0^H T_{\text{fin}}(\zeta)\,\mathrm{d}\zeta \tag{45}$$

The above descriptive equations were solved using the finite volume method. The solution process was iterative with a sequence of solving firstly T_b and T_{fin}, and then T_f. Each equation was discretized over its individual computational domain, leading to a set of algebraic equations for each variable. The sets of algebraic equations for all the variables were then solved by the line-by-line procedure, which is a combination of the tridiagonal matrix algorithm and the Gauss–Seidel iteration technique of Patankar [24]. The numerical program was coded in FORTRAN, and the typical computing time for one run was about 1 h on a personal computer.

V. Discussion of Results: Case Study

In Sec. III, an analytical model based on thermal resistance analogy has been developed to estimate the local temperature of the hottest region on the substrate of pin-fin heat sinks subjected to nonuniform flame impinging jet. The model is dependent upon many design parameters such as mass flow rate of convection flow, thermal conductivities of solid and fluid phases, channel height and length, pin-fin geometrical parameters, and substrate thickness. The applicability of the model in the design of pin-fin heat sinks is considered in this section by performing a case study. The prediction results of the analogy model are compared with those from the numerical model detailed in Sec. IV to verify the suitability of the assumptions/approximations made in the analogy model.

The nonuniform distribution of heat flux reported by Carbajal et al. [23] for flame jet impinging on a square plate is employed as the thermal loading in the case study. The empirical constants in Eq. (10) were determined by fitting the data in [23], as plotted in Fig. 7, and estimated to be $B=5$ and $C=2.6$ with $q_0=1.35\times10^5$ W/m^2 at $x/L=0$. Table 1 lists the geometrical parameters of the pin-fin heat sink considered. The substrate has dimensions 560 (W) by 560 (L) by 6.35 (t) in millimeters, identical to those of the sandwich heat pipe studied by Carbajal et al. [23].

With the thermal loading conditions fixed, amongst many other design parameters listed above, the mass flow rate of convective flow, the thermal conductivity of heat-sink material, and the thickness of the substrate are selected as variables in the case study to show the applicability of the model in the design of heat sinks. Whilst the first parameter is a typical factor influencing convective heat transfer from pin-fin heat sink to fluid flow, the other two parameters affect (lateral) conduction in the substrate playing a crucial role in the total thermal resistance for power chip cooling with discrete nonuniform heating.

A. Effect of Convective Flow Rate and Solid Thermal Conductivity

To quantify the influence of flow rate on the thermal performance of the pin-fin heat sink using the analogy model, the convective flow rate is varied from 0.07 kg/s to 0.46 kg/s (equivalently, Re_{Dh} ranging from 1×10^4 to 8×10^4), and it is assumed that the substrate

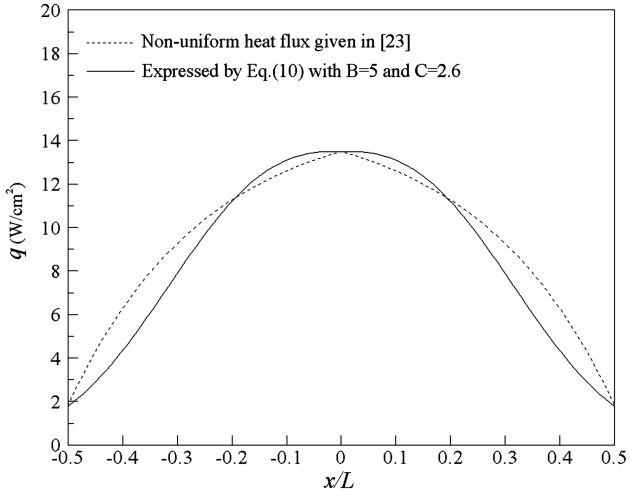

Fig. 7 Nonuniform heat flux distribution employed in case study.

and pin fins are made of aluminum (thermal conductivity $k_s = 237.3$ W/m K).

The total thermal resistance R_{tot}, the spreading resistance R_s, the material resistance R_m, the equivalent convective resistance R_{conv}, and the resistance caused by fluid temperature rise R_{heat} are plotted in Fig. 8 as a function of the mass flow rate. The dashed lines represent the results estimated by the numerical model, and the solid lines denote those predicted by the present analogy model.

With excellent agreement shown in Fig. 8, the predictions by both models show that the total thermal resistance is pronouncedly decreased as the mass flow rate is increased. This indicates that the local temperature on the substrate coinciding with the jet axis (i.e., impinging center) decreases with increasing the flow rate. With the rate of heat transfer from the substrate to coolant flow increased such as by increasing the flow rate, the heat concentrated on the substrate at $z = 0$ tends to be transported via the thickness of the substrate to $z = t$, rather than being spread laterally. As a consequence, the spreading resistance is found to reduce as the mass flow rate is increased, suggesting that the temperature distribution in the substrate becomes more uniform. In sharp contrast, the material resistance appears to be independent of the flow condition in the pin-fin channel.

Increasing the mass flow rate leads to increased equivalent endwall heat transfer coefficient and decreased fluid temperature rise in the pin-fin channel. Consequently, both the equivalent convective resistance and the resistance caused by fluid temperature rise decrease as observed in Fig. 8.

Consider next the effect of solid thermal conductivity k_s on the thermal resistances, R_{tot}, R_s, R_m, R_{conv}, and R_{heat}. Figure 9 plots the thermal resistances as functions of k_s at a fixed mass flow rate of 0.2322 kg/s ($\sim Re_{Dh} = 4 \times 10^4$). Increasing the thermal conductivity decreases the overall thermal resistance, which is attributable mainly to the decrease in the spreading resistance and partly to the decrease in material and convective resistances. For a highly conducting substrate such as aluminum or copper, the strong lateral conduction in the substrate transfers more heat from the region near the impinging center to the edge of the substrate ($r = r_0$ or $x = L/2$ and $y = W/2$). As a result, the spreading resistance decreases with increasing conductivity as the temperature distribution in the substrate becomes more uniform.

The decreased material resistance (R_m) as k_s is increased suggests that the temperature drop through the substrate thickness, $T_b(z = 0) - T_b(z = t)$, is reduced. The equivalent convective resistance (R_{conv}) decreases as k_s is increased till approximately 200 W/m K, beyond which R_{conv} becomes insensitive to k_s. The initial decrease in R_{conv} with increasing k_s is due to increased fin efficiency [see Eqs. (28) and (29)]: increase in equivalent endwall heat transfer coefficient and subsequent decrease in equivalent convective resistance.

Table 1 Geometrical parameters of pin-fin heat sink considered in case study

Substrate dimensions ($W \times L \times t$)	$560 \times 560 \times 6.35$ mm
Pin-fin height, H	51.3 mm
Pin-fin thickness, D	8 mm
Transverse/longitudinal fin pitch, S_T/S_L	18/18 mm
Transverse/longitudinal number of pin fins, N_T/N_L	30/30

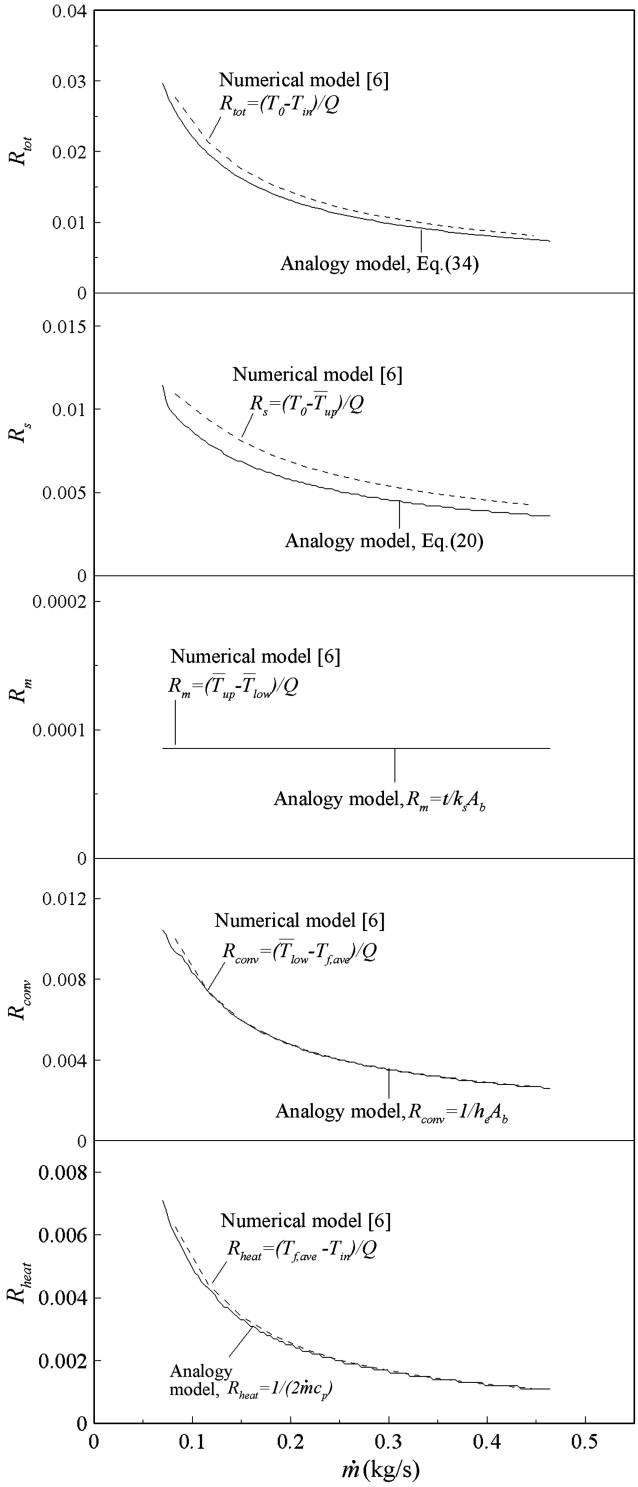

Fig. 8 Variations of R_{tot}, R_s, R_m, R_{conv} and R_{heat} with mass flow rate of forced convective flow in pin-fin heat sink ($k_s = 237.3$ W/m K).

With both the heat input and mass flow rate fixed, the fluid temperature rise in the pin-fin channel is also fixed, independent of k_s. Therefore, the resistance caused by the fluid temperature rise is not a function of k_s as indicated in Fig. 9.

As shown in Figs. 8 and 9, when comparing the results predicted by the analogy model and the numerical model, the overall trends of each individual thermal resistance are successfully predicted by the analogy model with mass flow rate and solid conductivity varied in a wide range. Quantitatively, the total thermal resistance is about 8% underestimated compared with the numerical model. This is mainly contributed to the underestimated spreading resistance R_s (~15%), and each of the other individual resistances (including R_m, R_{conv}, and R_{heat}) agrees well between the two models. The underestimation of the spreading resistance is associated with the assumptions/approximations made when deriving the spreading resistance. First, the reference fluid temperature $T_{f,\text{ave}}$ is assumed to be uniform beneath the substrate, whereas it is actually distributed in the channel with the in-plane distribution characterized by C-type isothermals under nonuniform impingement heating [6]. The local fluid temperature distribution will inversely influence the local temperature distribution in the substrate and then the spreading resistance. Second, the circular plate (2-D axisymmetric model) is used replacing the rectangular plate (3-D model) when deriving R_s. Finally, the local constriction resistance near each pin-fin end is ignored in the analogy model; i.e., the temperature of the substrate over unfinned surface is assumed the same as that over pin-fin root in each pin-fin unit cell for the analogy model; in contrast, the numerical model is able to predict the detailed temperature distribution of the substrate such as the thermal footprints of pin fins. Despite such simplifications, the present thermal resistance model provides results with acceptable accuracy, requiring no complex and exhaustive calculations.

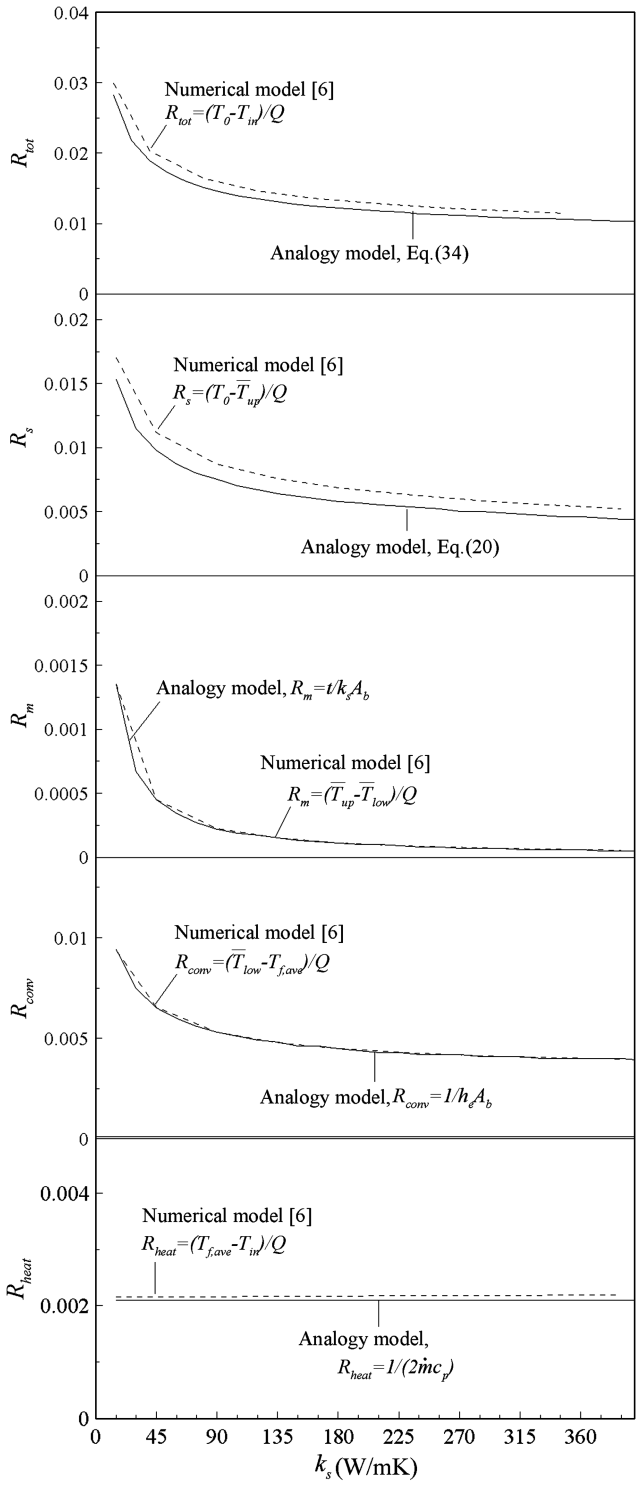

Fig. 9 Variations of R_{tot}, R_s, R_m, R_{conv}, R_{heat} with solid thermal conductivity at $Re_{Dh} = 4 \times 10^4$.

With the substrate thickness fixed (Table 1), the results of Figs. 8 and 9 also demonstrate that for a wide range of mass flow rate and solid conductivity, the spreading resistance contributes as large as 40–56% to the total thermal resistance. Therefore, reducing the spreading resistance is important if the total thermal resistance is to be reduced.

B. Optimal Substrate Thickness

Besides solid conductivity, the thickness of the substrate is another factor affecting the lateral spreading of heat in the substrate. Increasing the substrate thickness widens the path for lateral heat spreading, hence decreasing the spreading resistance; conversely, the material resistance along the thickness direction increases with increasing substrate thickness. As lateral heat spreading competes with that conducted through the thickness direction, an optimal substrate thickness minimizing substrate temperature at impinging center should exist. In fact, for electronics cooling with discrete nonuniform heating, the optimal substrate thickness is found to be of the order of the chip size [14,25].

From the analysis in Sec. III, one finds that only the spreading resistance and material resistance are changed as the substrate thickness is varied, but not the equivalent convective resistance and the thermal resistance caused by fluid temperature rise. Both the spreading resistance and material resistance are dependent upon heat conduction in the substrate. The optimal thickness is found by minimizing the sum of the two resistances (referred to as the substrate resistance below):

$$R_{\text{sub}} = R_s + R_m \tag{46}$$

Substituting Eqs. (20) and (22) into (46), one can write the dimensionless substrate resistance as

$$\Psi_{\text{sub}} = k_s r_0 R_{\text{sub}} = \frac{\tau}{\pi} + \Psi_s \tag{47}$$

which is a function of dimensionless substrate thickness, Biot number, B, and C [see Eqs. (20) and (21)]: i.e.,

$$\Psi_{\text{sub}} = fn(\tau, Bi, B, C) \tag{48}$$

For the pin fins considered in Table 1, if these are made of aluminum ($k_s \sim 237.3$ W/m K), the equivalent endwall heat transfer coefficient h_e varies from 300 W/m^2 K to 1500 W/m^2 K as predicted with Eq. (30) when the forced air flow velocity varies from 2 m/s to 20 m/s (Re_{Dh} from 1×10^4 to 1.2×10^5). The equivalent radius of the substrate of the considered heat sink is $r_0 = 0.316$ m; hence, the corresponding Biot number Bi varies from 0.4 to 2. In some extreme cases, such as natural convection cooling and two-phase convective boiling, the heat transfer coefficient h_e may change dramatically, on the order of 10 W/m^2 K for natural convection and 10,000 W/m^2 K for phase-change heat transfer

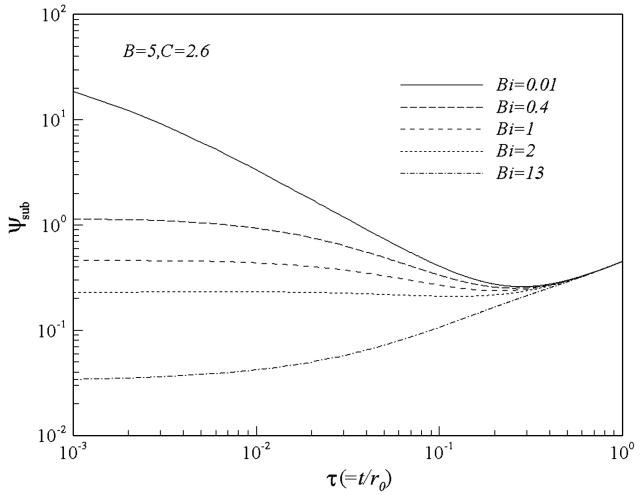

Fig. 10 Dimensionless substrate resistance plotted as a function of dimensionless substrate thickness τ for selected Biot numbers, with $B = 5$ and $C = 2.6$.

[26]; correspondingly, the Biot numbers for the two extreme cases are about 0.01 and 13, respectively.

Figure 10 presents the dimensionless substrate resistance as a function of dimensionless substrate thickness with $B = 5$ and $C = 2.6$ for a wide range of Biot numbers spanning from natural convection via forced convection to two-phase boiling heat transfer. As shown in Fig. 10, an optimal substrate thickness exists at $\sim\tau = 0.20$, when $Bi \leq 2$ for typical natural convection and forced air convection cooling of pin fins. Lateral spreading of heat dominates heat conduction in the substrate when the substrate thickness is smaller than the optimal value, whereas the reverse holds when the substrate thickness exceeds the optimal value. The results of Fig. 10 demonstrate that the initial increase in substrate thickness is sufficient to decrease the substrate resistance for relatively low Biot numbers, but the effect is increasingly diminished as the Biot number is increased. This is because heat tends to flow directly through the thickness direction, rather than spread out at relatively high Biot numbers, as previously mentioned.

When the Biot number becomes sufficiently large (e.g., 13), corresponding to phase-change cooling, the increase in substrate thickness leads to the monotonic increasing of substrate resistance. Practically, this indicates that, for example, for a flat sandwich heat pipe [22,23] subjected to nonuniform flame impinging-jet heating where phase-change heat transfer occurs at the evaporator substrate (heated substrate), a thinner substrate is beneficial for obtaining a lower temperature on the heated substrate. In this case, the substrate acts as an insulator, the substrate resistance continuously increases as the substrate thickness is increased, and hence no optimal substrate thickness exists (Fig. 10). Note, however, that so far we have ignored the strong influence of thickness on the structural properties of the substrate which, obviously, cannot be arbitrarily thin if the substrate is required to carry structural loading and to dissipate heat.

VI. Conclusions

The concept of thermal resistance analogy is employed to develop an engineering-level analytical model for the complicated heat transfer problem: pin-fin heat sink subjected to nonuniform flame impinging-jet heating. The assumptions/approximations made in the analogy model are verified by comparing model predictions with the results obtained from an analytically developed numerical model that is free from all the assumptions/approximations. The predicted overall trends of the thermal resistances agree well with the numerical model; quantitatively, the total thermal resistance is underestimated, about 8% lower than that from the numerical model over a wide range of convective flow rate and thermal conductivity of heat-sink material considered. Compared with tedious numerical simulation, the simple analogy model is valuable for fast calculation during the early stage of heat-sink design with acceptable accuracy.

In addition to increasing the material conductivity of the substrate and its thickness, the spreading resistance can also be reduced by increasing the rate of convective heat transfer from the substrate to the fluid flow (e.g., by increasing the convective flow rate). In this case, rather than being spread laterally, the concentrated heat on the substrate at surface $z = 0$ tends to be transported in the thickness direction of the substrate to surface $z = t$, where it is dissipated to the convective coolant flow. It can be safely concluded that the spreading effect diminishes as the convective heat transfer in the channel is enhanced.

An optimal substrate thickness minimizing the temperature at the impinging center is found to exist with all other parameters fixed. The optimal substrate thickness is about a fifth of the equivalent radius of the substrate, when the Biot number has a value less than 2 (corresponding to low heat transfer coefficient and high thermal conductivity). When $Bi > 2$ (high heat transfer coefficient and low conductivity), the substrate acts thermally as an insulator and its thickness cannot be optimized.

Acknowledgments

This work is supported by the National Basic Research Program of China (2006CB601203), the National Natural Science Foundation of China (10825210), and the National 111 Project of China (B06024).

References

[1] Tahat, M., Kodah, Z. H., Jarrah, B. A., and Probert, S. D., "Heat Transfers from Pin-Fin Arrays Experiencing Forced Convection," *Applied Energy*, Vol. 67, 2000, pp. 419–442. doi:10.1016/S0306-2619(00)00032-5

[2] Sara, O. N., Yapici, S., Yilmaz, M., and Pekdemir, T., "Second Law Analysis of Rectangular Channels with Square Pin-Fins," *International Communications in Heat and Mass Transfer*, Vol. 28, No. 5, 2001, pp. 617–630. doi:10.1016/S0735-1933(01)00266-4

[3] Sara, O. N., "Performance Analysis of Rectangular Ducts with Staggered Square Pin Fins," *Energy Conversion and Management*, Vol. 44, 2003, pp. 1787–1803. doi:10.1016/S0196-8904(02)00185-1

[4] Kim, D., Kim, S. J., and Ortega, A., "Compact Modeling of Fluid Flow and Heat Transfer in Pin Fin Heat Sinks," *Journal of Electronic Packaging*, Vol. 126, 2004, pp. 342–350. doi:10.1115/1.1772415

[5] Jeng, T. M., and Tzeng, S. C., "Pressure Drop and Heat Transfer of Square Pin-Fin Arrays in In-line and Staggered Arrangements," *International Journal of Heat and Mass Transfer*, Vol. 50, 2007, pp. 2364–2375. doi:10.1016/j.ijheatmasstransfer.2006.10.028

[6] Feng, S. S., Kim, T., and Lu, T. J., "A Semi-Empirical Heat Transfer Model for Forced Convection in Pin-Fin Heat Sinks Subjected to Non-Uniform Heating," *Journal of Heat Transfer*, Vol. 132, 2010, p. 121702. doi:10.1115/1.4002285

[7] Peles, Y., Kosar, Ali, Mishra, C., Kuo, C.-J., and Schneider, B., "Forced Convective Heat Transfer Across a Pin Fin Micro Heat Sink," *International Journal of Heat and Mass Transfer*, Vol. 48, 2005, pp. 3615–3627. doi:10.1016/j.ijheatmasstransfer.2005.03.017

[8] Khan, W. A., Culham, J. R., and Yovanovich, M. M., "Performance of Shrouded Pin-Fin Heat Sinks for Electronic Cooling," *Journal of Thermophysics and Heat Transfer*, Vol. 20, No. 3, 2006, pp. 408–414. doi:10.2514/1.17713

[9] Yovanovich, M. M., Muzychka, Y. S., and Culham, J. R., "Spreading Resistance of Isoflux Rectangles and Strips on Compound Flux Channels," *Journal of Thermophysics and Heat Transfer*, Vol. 13, No. 4, 1999, pp. 495–500. doi:10.2514/2.6467

[10] Song, S., Lee, S., and Au, V., "Closed-Form Equation for Thermal Constriction/Spreading Resistances with Variable Resistance Boundary Condition," *Proceedings of the Technical Conference*, International Packaging Society, Wheaton, IL, 1994, pp. 111–121.

[11] Yovanovich, M. M., and Marotta, E., "Thermal Contact Resistance," *Heat Transfer Handbook*, edited by A. Bejan and A. D. Kraus, Wiley, New York, 2003, Chap. 4.

[12] Lee, S., Song, S., Au, V., and Moran, K. P., "Constriction/Spreading Resistance Model for Electronics Packaging," *Proceedings of the 4th ASME/JSME Thermal Engineering Joint Conference*, Vol. 4, American Society of Mechanical Engineers, New York, 1995, pp. 199–206.

[13] Kennedy, D. P., "Spreading Resistance in Cylindrical Semiconductor Devices," *Journal of Applied Physics*, Vol. 31, 1960, pp. 1490–1497. doi:10.1063/1.1735869

[14] Lu, T. J., Evans, A. G., and Hutchinson, J. W., "The Effects of Material Properties on Heat Dissipation in High Power Electronics," *Journal of Electronic Packaging*, Vol. 120, 1998, pp. 280–289. doi:10.1115/1.2792634

[15] Yovanovich, M. M., "Thermal Resistances of Circular Source on Finite Circular Cylinder with Side and End Cooling," *Journal of Electronic Packaging*, Vol. 125, 2003, pp. 169–177. doi:10.1115/1.1568124

[16] Yovanovich, M. M., Tien, C. H., and Schneider, G. E., "General Solution of Constriction Resistance Within a Compound Disk," *Heat Transfer, Thermal Control, and Heat Pipes*, AIAA Progress in Astronautics and Aeronautics, Vol. 70, AIAA, Reston, VA, 1980, pp. 47–62.

[17] Mikic, B. B., and Rohsenow, W. M., "Thermal Contact Resistance," Massachusetts Inst. of Technology, Mechanical Engineering Dept., Rept. DSR 74542-41, Cambridge MA, 1966.

[18] Negus, K. J., Yovanovich, M. M., and Beck, J. V., "On the Nondimensionalization of Constriction Resistance for Semi-Infinite Heat Flux Tubes," *Journal of Heat Transfer*, Vol. 111, 1989, pp. 804–807. doi:10.1115/1.3250755

[19] Nelson, D. J., and Sayers, W. A., "A Comparison of Two-Dimensional Planar, Axisymmetric and Three-Dimensional Spreading Resistances," *Proceedings of the 8th IEEE Semiconductor Thermal Measurement and Management Symposium*, Inst. of Electrical and Electronics Engineers, Piscataway, NJ, 1992, pp. 62–68.

[20] Naraghi, M. H. N., and Antonetti, V. W., "Macro-Constriction Resistance of Distributed Contact Contour Areas In a Vacuum Environment," *Enhanced Cooling Techniques for Electronics Applications*, Heat Transfer Div., American Society of Mechanical Engineers, Vol. 263, New York, 1993, pp. 107–114.

[21] Culham, J. R., Khan, W. A., Yovanovich, M. M., and Muzychka, Y. S., "The Influence of Material Properties and Spreading Resistance in the Thermal Design of Plate Fin Heat Sinks," *Journal of Electronic Packaging*, Vol. 129, 2007, pp. 76–81. doi:10.1115/1.2429713

[22] Carbajal, G., Sobhan, C. B., Peterson, G. P., Queheillalt, D. T., and Wadley, H. N. G., "Thermal Response of a Flat Heat Pipe Sandwich Structure to a Localized Heat Flux," *International Journal of Heat and Mass Transfer*, Vol. 49, 2006, pp. 4070–4081. doi:10.1016/j.ijheatmasstransfer.2006.03.035

[23] Carbajal, G., Sobhan, C. B., Peterson, G. P., Queheillalt, D. T., and Wadley, H. N. G., "A Quasi-3D Analysis of the Thermal Performance ofa Flat Heat Pipe," *International Journal of Heat and Mass Transfer*, Vol. 50, 2007, pp. 4286–4296. doi:10.1016/j.ijheatmasstransfer.2007.01.057

[24] Patankar, S. V., *Numerical Heat Transfer and Fluid Flow*, McGraw–Hill, New York, 1980.

[25] Hingorani, S., Fahrner, C. J., Mackowski, D. W., Gooding, J. S., and Jaeger, R. C., "Optimal Sizing of Planar Thermal Spreaders," *Journal of Heat Transfer*, Vol. 116, 1994, pp. 296–301. doi:10.1115/1.2911399

[26] Chen, Y. S., Chien, K. H., Wang, C. C., Hung, T. C., Ferng, Y. M., and Pei, B. S., "Investigations of the Thermal Spreading Effects of Rectangular Conduction Plates and Vapor Chamber," *Journal of Electronic Packaging*, Vol. 129, 2007, pp. 348–355. doi:10.1115/1.2753970